Electronic Supplementary Material (ESI) for Journal of Materials Chemistry A.

—Electronic Supplementary Information— The Resistive Nature of Decomposing Interfaces of Solid Electrolytes with Alkali Metal Electrodes

Juefan Wang,[†] Abhishek A. Panchal,[†] Gopalakrishnan Sai Gautam,[‡] and Pieremanuele Canepa[*,†,¶]

[†]*Department of Materials Science and Engineering, National University of Singapore, 9 Engineering Drive 1, 117575, Singapore*

[‡]*Department of Materials Engineering, Indian Institute of Science, Bangalore 560012, India*

[¶]*Department of Chemical and Biomolecular Engineering, National University of Singapore, 4 Engineering Drive 4, 117585, Singapore*

E-mail: pcanepa@nus.edu.sg

Contents

S1 Bulk Structures **ESI3**

S2 Surface Energies **ESI4**

S3 Interface Characteristics **ESI6**

S4 Alkali metal-anion bond lengths in interfaces **ESI7**

S5 MTP training and validation errors **ESI8**

S6 Activation energy for Binary Compounds **ESI9**

S7 MTP-MD calculated tracer diffusivity of interfaces **ESI9**

S8 AIMD calculated tracer diffusivity of interfaces **ESI10**

S9 Interface structures **ESI11**

References **ESI23**

S1 Bulk Structures

Table S1: Lattice parameters (in Å) as computed using the PBE functional and experimental (Exp.) measurements of alkali metals and their binary compounds.

Compound	Method	Space Group	Lattice Constants
		Li compounds	
Li	PBE	$Im\bar{3}m$	3.44
Li	Exp.	$Im\bar{3}m$	3.48
Li_2S	PBE	$Fm\bar{3}m$	5.71
Li_2S	Exp.	$Fm\bar{3}m$	5.69
Li_3P	PBE	$P6_3/mmc$	4.23, 7.56
Li_3P	Exp.	$P6_3/mmc$	4.27, 7.59
LiCl	PBE	$Fm\bar{3}m$	5.15
LiCl	Exp.	$Fm\bar{3}m$	5.13
Li_2O	PBE	$Fm\bar{3}m$	4.64
Li_2O	Exp.	$Fm\bar{3}m$	4.60–4.70
Li_3N	PBE	$P6/mmm$	3.64, 3.87
Li_3N	Exp.	$P6/mmm$	3.65, 3.88
		Na compounds	
Na	PBE	$Im\bar{3}m$	4.19
Na	Exp.	$Im\bar{3}m$	4.23
Na_2S	PBE	$Fm\bar{3}m$	6.54
Na_2S	Exp.	$Fm\bar{3}m$	6.53
Na_3P	PBE	$P6_3/mmc$	4.95, 8.82
Na_3P	Exp.	$P6_3/mmc$	4.95, 8.79
Na_2O	PBE	$Fm\bar{3}m$	4.54
Na_2O	Exp.	$Fm\bar{3}m$	4.49

S2 Surface Energies

Table S2: Computed low-indexed surface energies (in J m^{-2}) of lithium binary compounds. Selected low-indexed surfaces are non-polar, containing symmetry (at least an inversion symmetry element) and stoichiometric. The termination of the surface is also shown.

Compound	Miller Index	Termination	γ
Li	100	Li	0.46
	110	Li	0.50
Li_2S	111	Li	0.33
	110	Li & S	0.51
	211	Li & S	0.72
Li_3P	001	Li	0.48
	101	Li	0.67
	110	Li & P	0.72
	211	Li & P	0.75
	221	Li & P	0.79
	212	Li & P	0.85
	102	Li & P	0.86
	201	Li & P	0.87
	111	Li & P	0.89
	100	Li & P	1.39
LiCl	100	Li & Cl	0.12
	210	Li & Cl	0.21
	110	Li & Cl	0.30
	221	Li & Cl	0.31
	211	Li & Cl	0.38
Li_2O	111	Li	0.53
	110	Li & O	0.92
	211	Li & O	1.17
Li_3N	100	Li	0.52
	210	Li	0.71
	110	Li & N	0.81
	102	Li	1.01
	212	Li	1.09
	$2\bar{1}2$	Li & N	1.24

Table S3: Computed low-indexed surface energies (in J m^{-2}) of sodium binary compounds. Selected low-indexed surfaces are non-polar, containing symmetry (at least an inversion symmetry element) and stoichiometric. The termination of the surface is also shown.

Compound	Miller Index	Termination	γ
Na	100	Na	0.22
	110	Na	0.21
Na_2S	111	Na	0.26
	110	Na & S	0.40
	211	Na & S	0.55
Na_3P	001	Na	0.33
	201	Na & P	0.38
	101	Na	0.39
	211	Na & P	0.42
	110	Na & P	0.43
	221	Na & P	0.46
	212	Na & P	0.47
	111	Na & P	0.51
	102	Na & P	0.52
	100	Na & P	0.78
Na_2O	111	Na	0.35
	110	Na & O	0.60
	211	Na & O	0.76

S3 Interface Characteristics

Table S4: Computed interfacial energy quantitites and other parameters of selected interfaces. Upon construction of heterogeneous interfaces, in models Li(100)||Li_2S(111), Li(100)||Li_2O(111), Li(110)||Li_2O(111) and Na(100)||Na_2S(111) the lattice misfit is in the binary compound, while in the remaining surfaces the lattice misfit appears in Li or Na metal. The calculated interface formation energy E_f (Eq. 2 in the main manuscript), the interfacial energy σ (Eq. 3), and the work of adhesion W_{adhesion} (Eq. 4) of the interfaces are expressed in J m^{-2}.

Interface	Dimensions	Mismatch	E_f	σ	$W_{adhesion}$
Li||LiX (X=Cl, O, N, S and P) interfaces					
Li(110)||Li_2S(110)	3×5/2×3 (γ=70.53°)	5.10	0.565	0.462	0.545
Li(100)||Li_2S(111)	4×4/2×2 (γ=62.47°)	14.17	0.423	0.319	0.470
Li(100)||Li_3P(001)	$2\times3/\sqrt{3}\times\sqrt{5}$ (γ=70.04°)	6.14	0.326	0.261	0.675
Li(110)||LiCl(100)	1×3/1×2 (γ=90.00°)	5.55	0.493	0.507	0.115
Li(100)||LiCl(100)	3×3/2×2 (γ=90.00°)	0.19	0.521	0.544	0.045
Li(100)||LiCl(110)	4×5/2×3 (γ=64.76°)	2.96	0.543	0.528	0.237
Li(110)||LiCl(110)	3×3/2×2 (γ=90.00°)	0.20	0.503	0.535	0.263
Li(100)||Li_2O(111)	4×4/2×2 (γ=62.47°)	7.37	0.655	0.627	0.359
Li(110)||Li_2O(111)	4×5/3×3 (γ=61.02°)	1.73	0.732	0.706	0.323
Li(100)||Li_2O(110)	2×4/1×3 (γ=90.00°)	5.00	0.403	0.362	1.010
Li(110)||Li_2O(110)	4×4/3×3 (γ=90.00°)	1.00	0.588	0.563	0.853
Li(100)||Li_3N(100)	4×5/4×4 (γ=64.82°)	2.82	0.284	0.249	0.723
Li(110)||Li_3N(100)	1×3/1×4 (γ=64.76°)	5.72	0.387	0.192	0.823
Li(100)||Li_3N(110)	5×5/4×3 (γ=67.85°)	2.91	0.276	0.235	1.034
Li(110)||Li_3N(110)	3×5/4×3 (γ=90.00°)	9.01	0.329	0.312	1.000
Na||NaX (X=O, S, and P) interfaces					
Na(110)||Na_2S(110)	3×3/2×2 (γ=90.00°)	3.80	0.315	0.308	0.302
Na(100)||Na_2S(111)	4×4/2×2 (γ= 61.93°)	6.97	0.340	0.307	0.175
Na(100)||Na_3P(001)	$2\times4/\sqrt{3}\times\sqrt{7}$ (γ= 76.10°)	3.27	0.192	0.191	0.362
Na(100)||Na_2O(110)	2×4/1×3 (γ= 90°)	7.00	0.262	0.220	0.606
Na(110)||Na_2O(110)	1×2/1×1 (γ= 90°)	7.01	0.278	0.177	0.650

S4 Alkali metal-anion bond lengths in interfaces

Table S5: Comparison between the Li-anion bond length in binary compounds, a (Å) and the bond length formed by Li(or Na) atoms within the first few layers of Li(or Na)-metal with anion species in the relaxed interfaces, b(Å)

Structure	a (Å)	b (Å)
Li/LiX (X=Cl, O, N, S and P) interfaces		
Li(110)||Li_2S(110)	2.47	2.35-2.74
Li(100)||Li_2S(111)	2.47	2.38–2.55
Li(100)||Li_3P(001)	2.44-2.75	2.50–2.56
Li(110)||LiCl(100)	2.58	2.43–2.51
Li(100)||LiCl(100)	2.58	2.48–2.55
Li(100)||LiCl(110)	2.58	2.37–2.72
Li(110)||LiCl(110)	2.58	2.46–2.64
Li(100)||Li_2O(111)	2.0	1.90–2.05
Li(110)||Li_2O(111)	2.0	1.84–1.86
Li(100)||Li_2O(110)	2.0	1.86–1.87
Li(110)||Li_2O(110)	2.0	1.84–1.90
Li(100)||Li_3N(100)	2.1	1.90–1.96
Li(110)||Li_3N(100)	2.1	1.98–2.01
Li(100)||Li_3N(110)	2.1	1.95–2.18
Li(110)||Li_3N(110)	2.1	1.95–2.19
Na||NaX (X=O, S, and P) interfaces		
Na(110)||Na_2S(110)	2.80–3.00	2.60–2.80
Na(100)||Na_2S(111)	2.7–3.00	2.60–2.80
Na(100)||Na_3P(001)	2.86–3.23	2.80–3.00
Na(100)||Na_2O(110)	2.40	2.28
Na(110)||Na_2O(110)	2.40	2.29

S5 MTP training and validation errors

Table S6 compares the fitting and validation errors on energies (in meV/atom) and forces (in meV/Å) for the trained moment tensor potentials (MTPs) of the systems in this study.

Table S6: The fitting and validation mean absolute errors (MAE) on energies (in meV/atom) and forces (in meV/Å) for the trained moment tensor potentials (MTPs) of the systems in this study.

System	Training MAE(1000K)		Validation MAE			
			300K		500K	
	Energy	Force	Energy	Force	Energy	Force
Li metal and binary compounds						
Li	0.86	17.90	8.05	20.77	5.55	19.11
Li with V_{Li+}	0.87	18.29	7.44	20.12	3.59	18.29
Li_2S	0.34	11.84	0.33	5.38	0.52	7.34
Li_2S with V_{Li+}	0.32	17.41	0.42	11.87	0.30	13.40
Li_3P	0.38	18.52	1.30	9.55	0.91	12.30
Li_3P with V_{Li+}	0.45	19.33	1.30	11.00	1.00	13.33
LiCl with V_{Li+}	0.38	18.02	0.15	10.02	0.23	13.08
Interface structures						
Li(100)||Li_3P(100) with V_{Li+}	0.64	25.53	0.43	17.45	1.14	19.40
Li(110)||Li_2S(110) with V_{Li+}	0.73	28.42	0.85	19.52	0.68	20.99
Li(110)||LiCl(100) with V_{Li+}	0.84	31.26	0.68	20.01	0.68	22.98

S6 Activation energy for Binary Compounds

Table S7: Computed activation energies E_a with the estimated standard errors (stderr) for the binary compounds in this study.

System	MTP-MD E_a ± stderr (eV)	Experimental E_a (eV)
Li	0.13 ± 0.014	
Li with V_{Li+}	0.13 ± 0.026	
Li_2S	1.57 ± 0.104	0.70 (T < 800 K), 1.52 (T > 800 K)[1]
Li_2S with V_{Li+}	0.31 ± 0.002	
Li_3P	1.06 ± 0.053	0.18[2]
Li_3P with V_{Li+}	0.15 ± 0.007	
LiCl with V_{Li+}	0.40 ± 0.005	0.51[3]

S7 MTP-MD calculated tracer diffusivity of interfaces

Table S8: MTP-MD calculated tracer diffusivity (cm^2/s) for Li^+ in Li(100)||Li_3P(001), Li(110)||Li_2S(110) and Li(110)||LiCl(100) interfaces.

T(K)	Li(100)||Li_3P(001)		Li(110)||Li_2S(110)		Li(110)||LiCl(100)	
	Li^+(metal)	Li^+(binary)	Li^+(metal)	Li^+(binary)	Li^+(metal)	Li^+(binary)
1000	9.80×10^{-5}	7.70×10^{-5}	–	–	1.28×10^{-4}	1.15×10^{-4}
900	7.49×10^{-5}	6.26×10^{-5}	8.74×10^{-5}	9.71×10^{-5}	9.07×10^{-5}	1.00×10^{-4}
800	5.64×10^{-5}	5.40×10^{-5}	5.93×10^{-5}	5.46×10^{-5}	7.12×10^{-5}	4.36×10^{-5}
700	3.90×10^{-5}	2.98×10^{-5}	4.49×10^{-5}	3.98×10^{-5}	5.58×10^{-5}	3.66×10^{-5}
600	2.27×10^{-5}	2.13×10^{-5}	3.73×10^{-5}	2.17×10^{-5}	2.44×10^{-5}	9.13×10^{-6}
500	1.25×10^{-5}	1.12×10^{-5}	2.79×10^{-5}	8.08×10^{-6}	7.60×10^{-6}	9.26×10^{-8}
400	3.76×10^{-6}	3.03×10^{-6}	1.89×10^{-7}	4.86×10^{-8}	1.15×10^{-6}	1.81×10^{-9}
300	5.11×10^{-7}	2.49×10^{-7}	4.08×10^{-8}	3.19×10^{-9}	2.99×10^{-10}	2.94×10^{-10}

S8 AIMD calculated tracer diffusivity of interfaces

Table S9: AIMD calculated tracer diffusivity (cm^2/s) for Li^+ in Li(100)||Li_3P(001), Li(110)||Li_2S(110) and Li(110)||LiCl(100) interfaces.

T (K)	Li(100)||Li_3P(001)	Li(110)||Li_2S(110)	Li(110)||LiCl(100)
1000	1.02×10^{-4}	1.41×10^{-4}	1.73×10^{-4}
900	7.78×10^{-5}	1.16×10^{-4}	1.23×10^{-4}
800	6.07×10^{-5}	1.02×10^{-4}	1.19×10^{-4}

S9 Interface structures

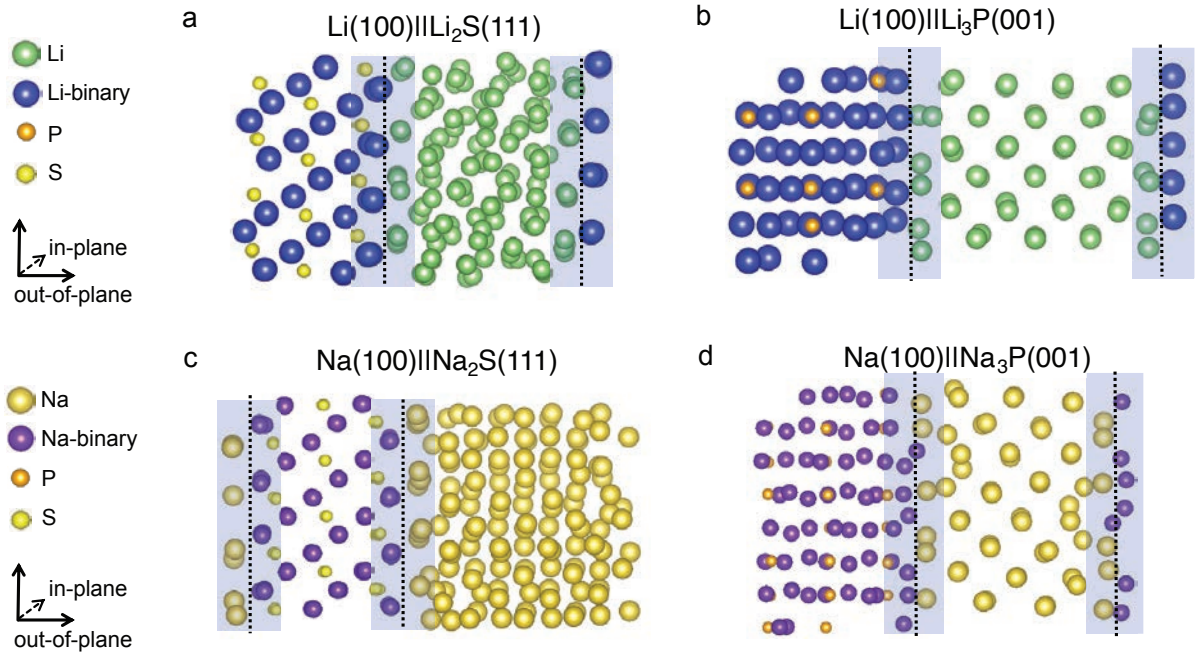

Figure S1: Atomic structures of fully relaxed interfaces, (a) Li(100)||Li_2S(111), (b) Li(100)||Li_3P(001), (c) Na(100)||Na_2S(111) and (d) Na(100)||Na_3P(001). The interface regions are indicated by violet shaded areas. The non-periodic direction of the interface is indicated by the "out-of-plane" vectors.

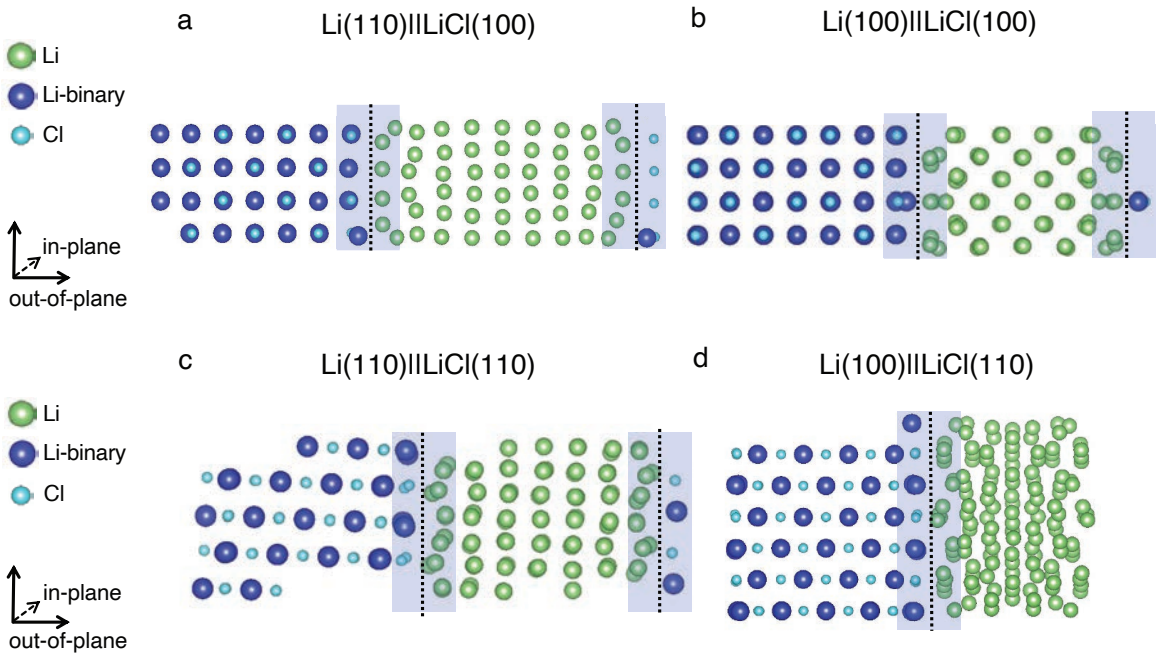

Figure S2: Atomic structures of fully relaxed interfaces, (a) Li(110)||LiCl(100), (b) Li(100)||LiCl(100), (c) Li(110)||LiCl(110) and (d) Li(100)||LiCl(110). The interface regions are indicated by violet shaded areas. The non-periodic direction of the interface is indicated by the "out-of-plane" vectors.

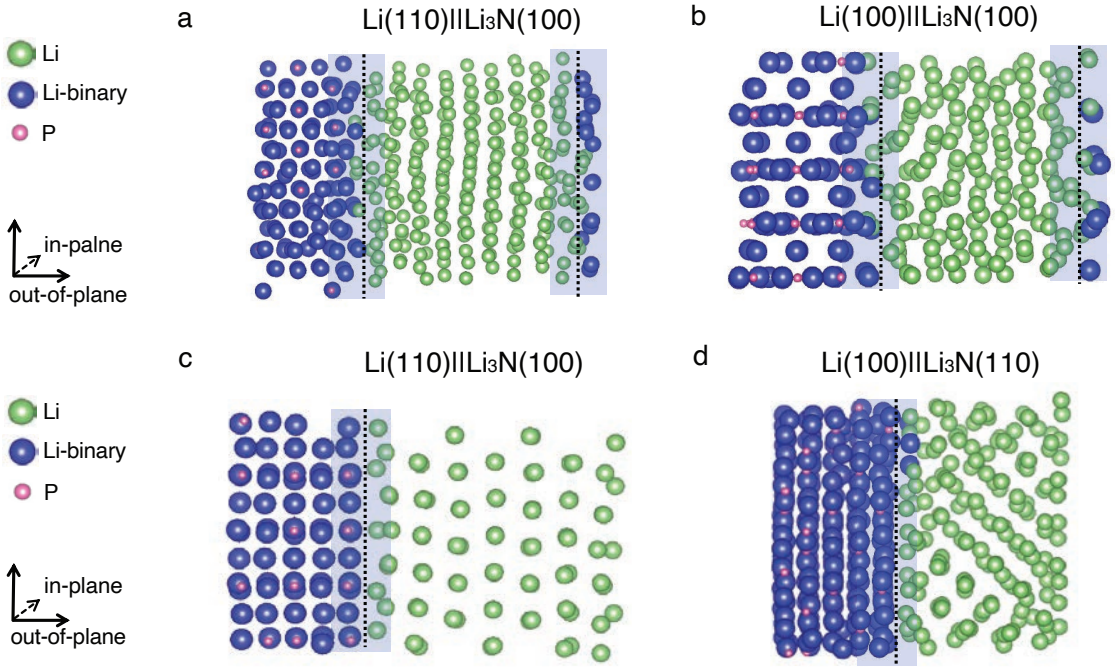

Figure S3: Atomic structures of fully relaxed interfaces, (a) Li(110)||Li_3N(100), (b) Li(100)||Li_3N(100), (c) Li(110)||Li_3N(110) and (d) Li(100)||Li_3N(110). The interface regions are indicated by violet shaded areas. The non-periodic direction of the interface is indicated by the "out-of-plane" vectors.

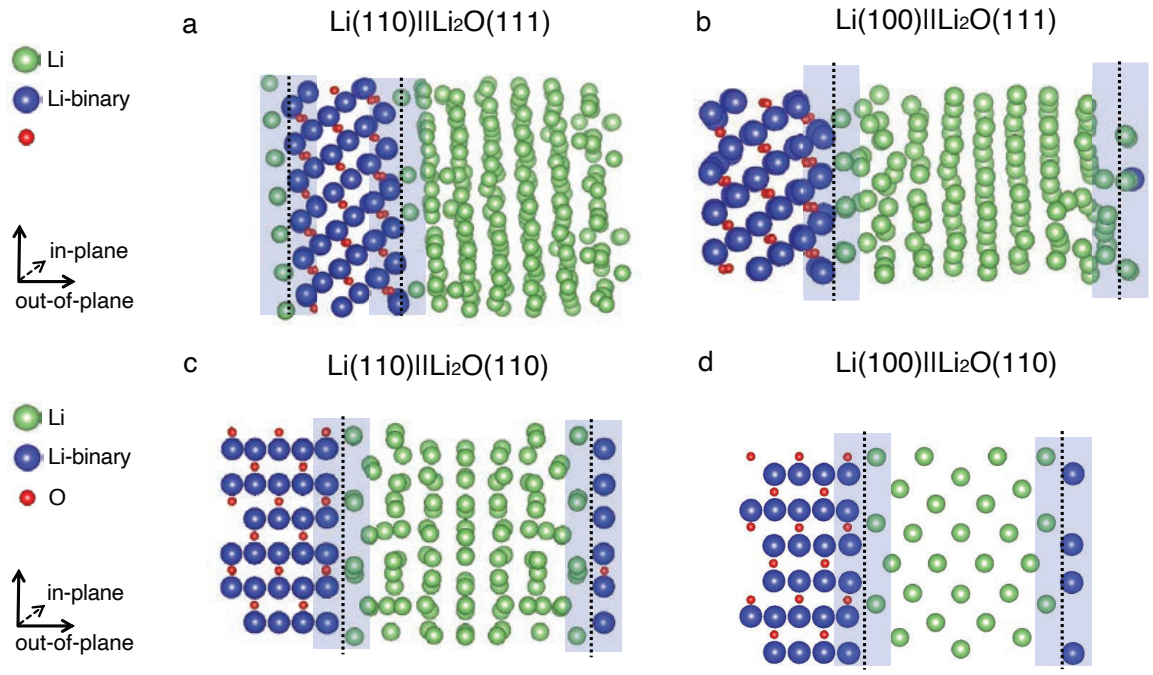

Figure S4: Atomic structures of fully relaxed interfaces, (a) Li(110)||Li_2O(111), (b) Li(100)||Li_2O(111), (c) Li(110)||Li_2O(110) and (d) Li(100)||Li_2O(110). The interface regions are indicated by violet shaded areas. The non-periodic direction of the interface is indicated by the "out-of-plane" vectors.

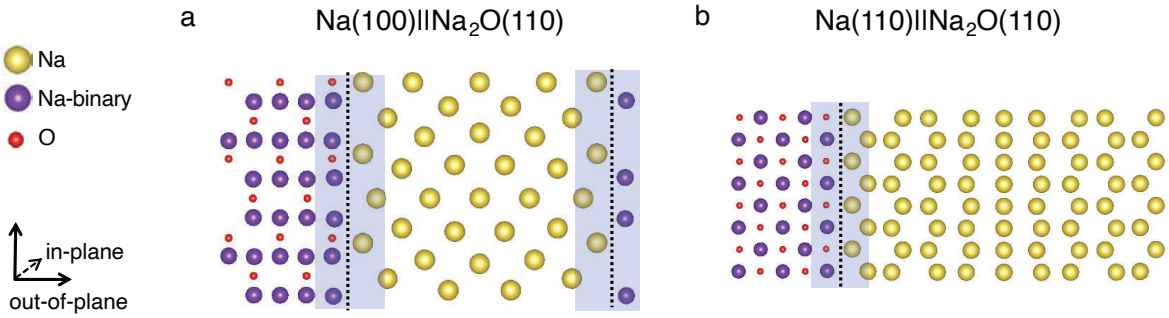

Figure S5: Atomic structures of fully relaxed interfaces, (a) Na(100)||Na_2O(110) and (b) Na(110)||Na_2O(110). The interface regions are indicated by violet shaded areas. The non-periodic direction of the interface is indicated by the "out-of-plane" vectors.

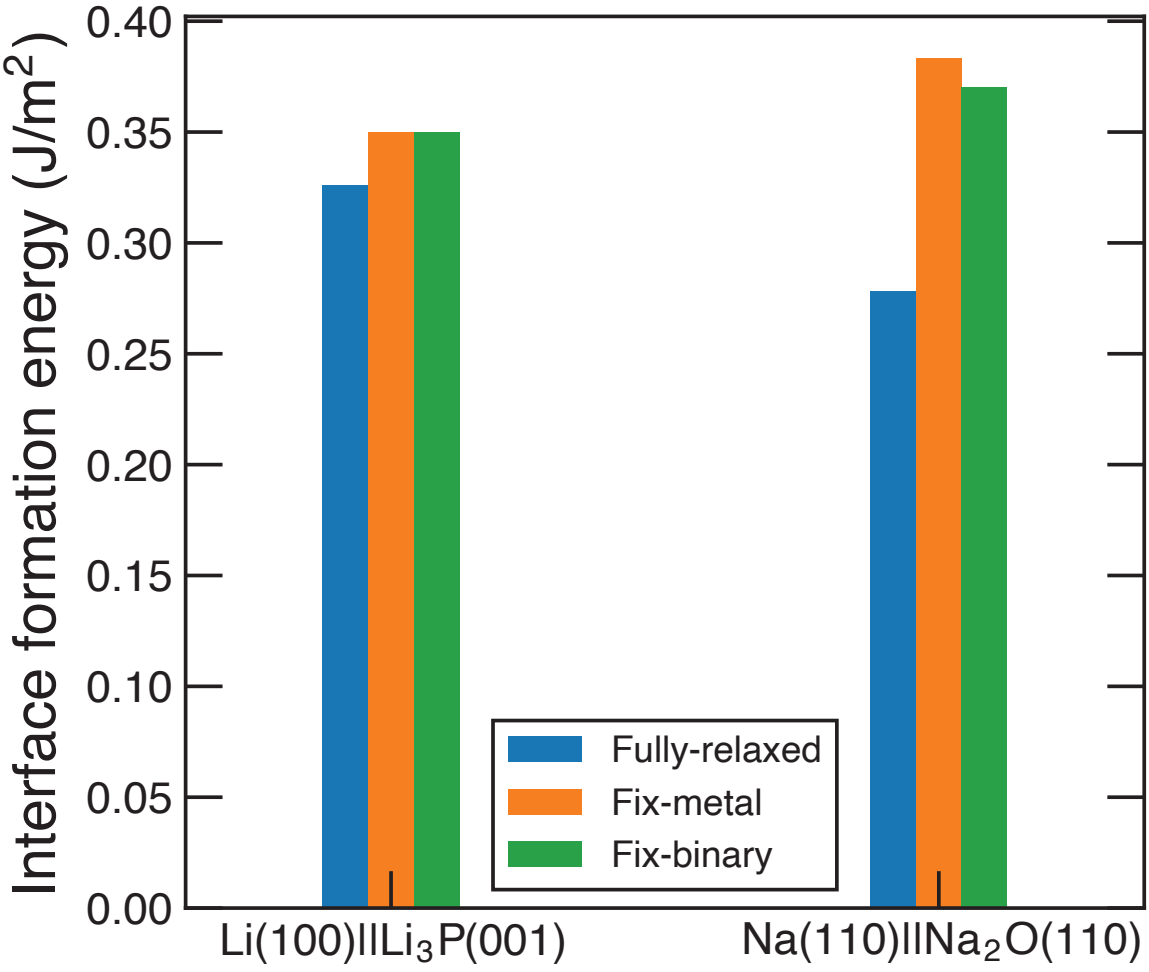

Figure S6: The calculated interface formation energy, E_f (J m^{-2}) using different methods. Fully-relaxed: fully relaxation for interface structure; Fix-metal: constrained relaxation for interface structure using the in-plane lattice constants of binary compound, fix the middle layers of the Li(or Na) metal; Fix-binary: constrained relaxation for interface structure using the in-plane lattice constants of binary compound, fix the middle layers of the binary compound.

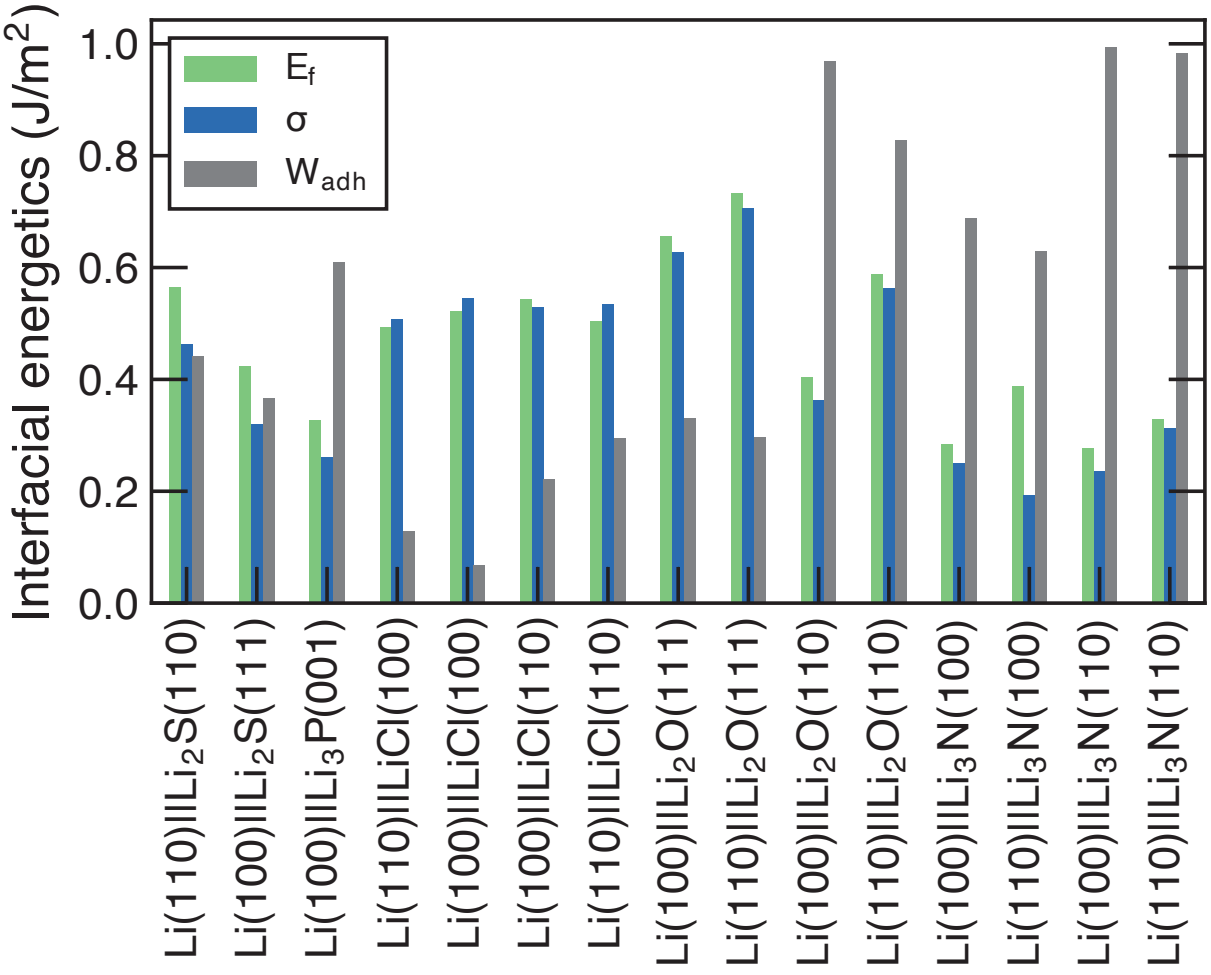

Figure S7: The calculated interfacial energetics (in J m^{-2}) for Li-based interfaces. The values of work of adhesion are calculated by using Eq. 5 of the main text.

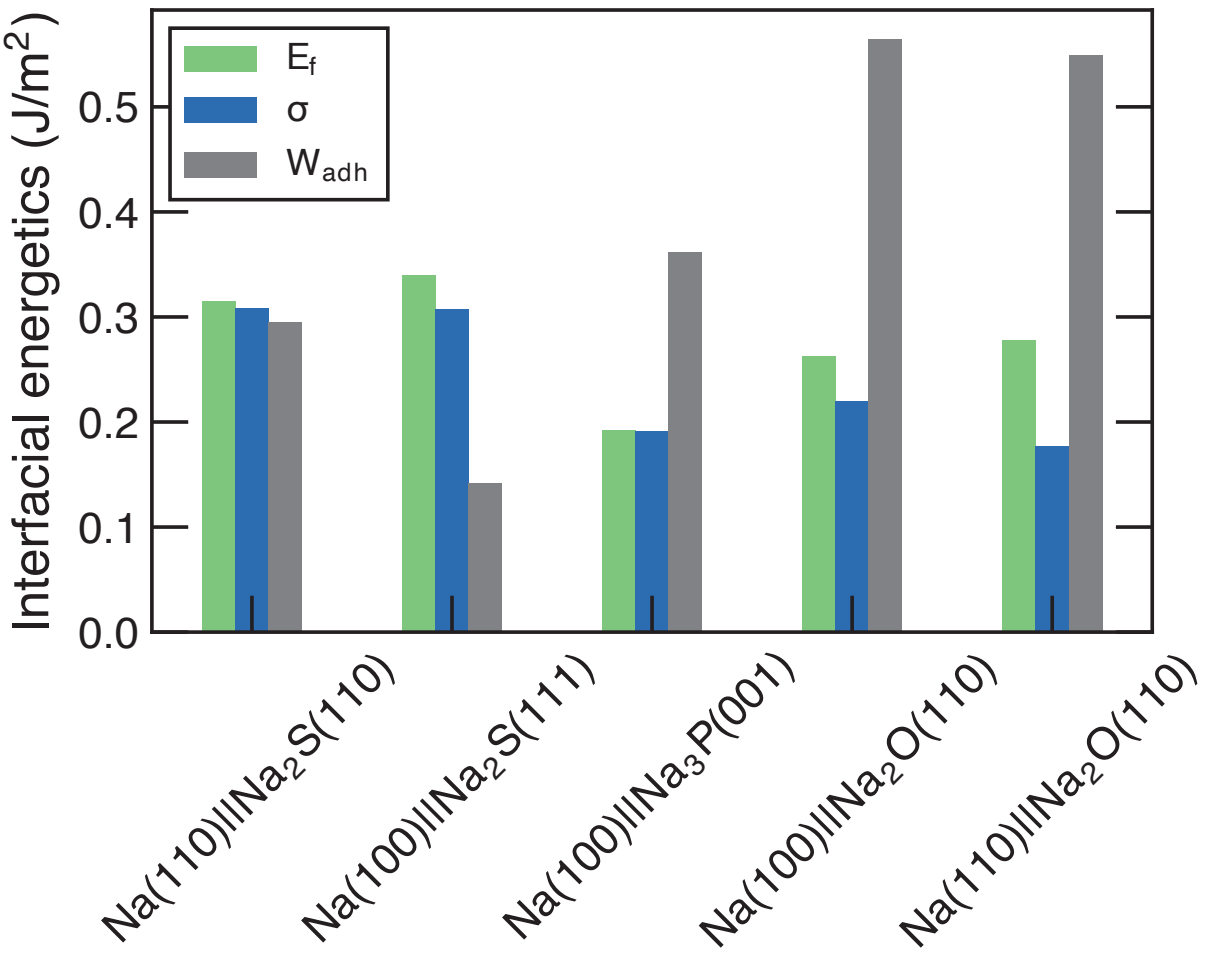

Figure S8: The calculated interfacial energetics (in J m^{-2}) for Na-based interfaces. The values of work of adhesion are calculated by using Eq. 5 of the main text.

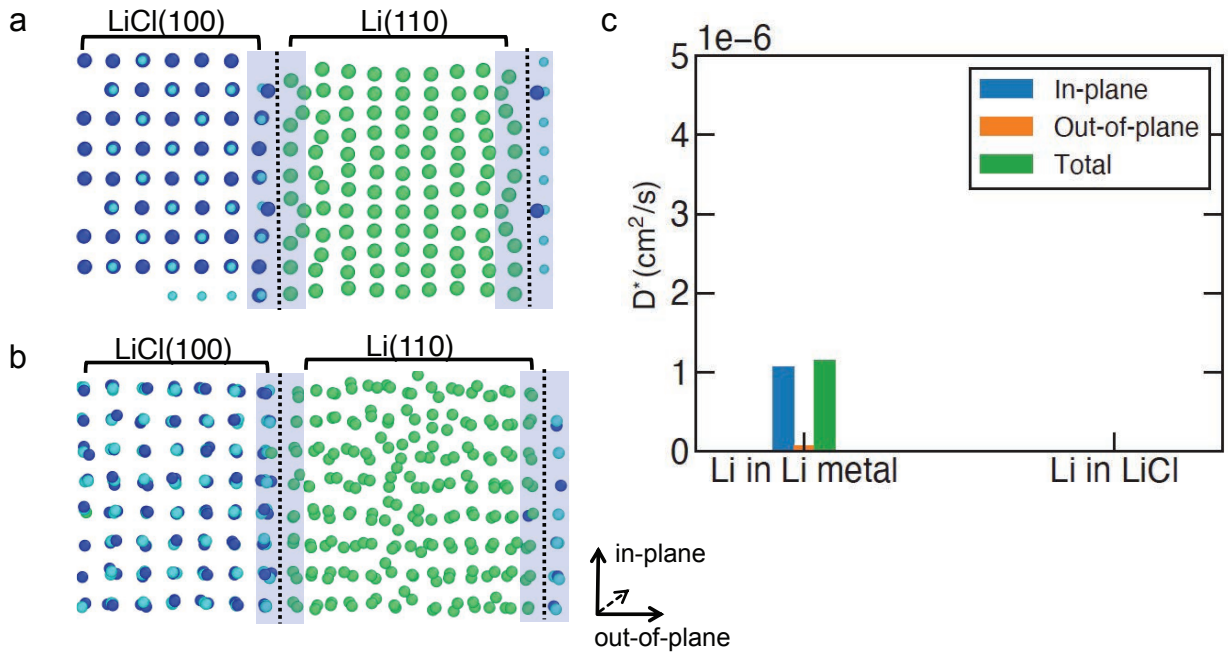

Figure S9: Snapshots of Li(110)||LiCl(100) interface (400 K) at (a) 0 ns and (b) 5 ns. (c) The in-plane and out-of-plane components of Li ion tracer diffusivity in the Li metal and LiCl regions at 400 K. Dark blue spheres: Li(binary), green spheres: Li(metal) and cyan spheres: Cl.

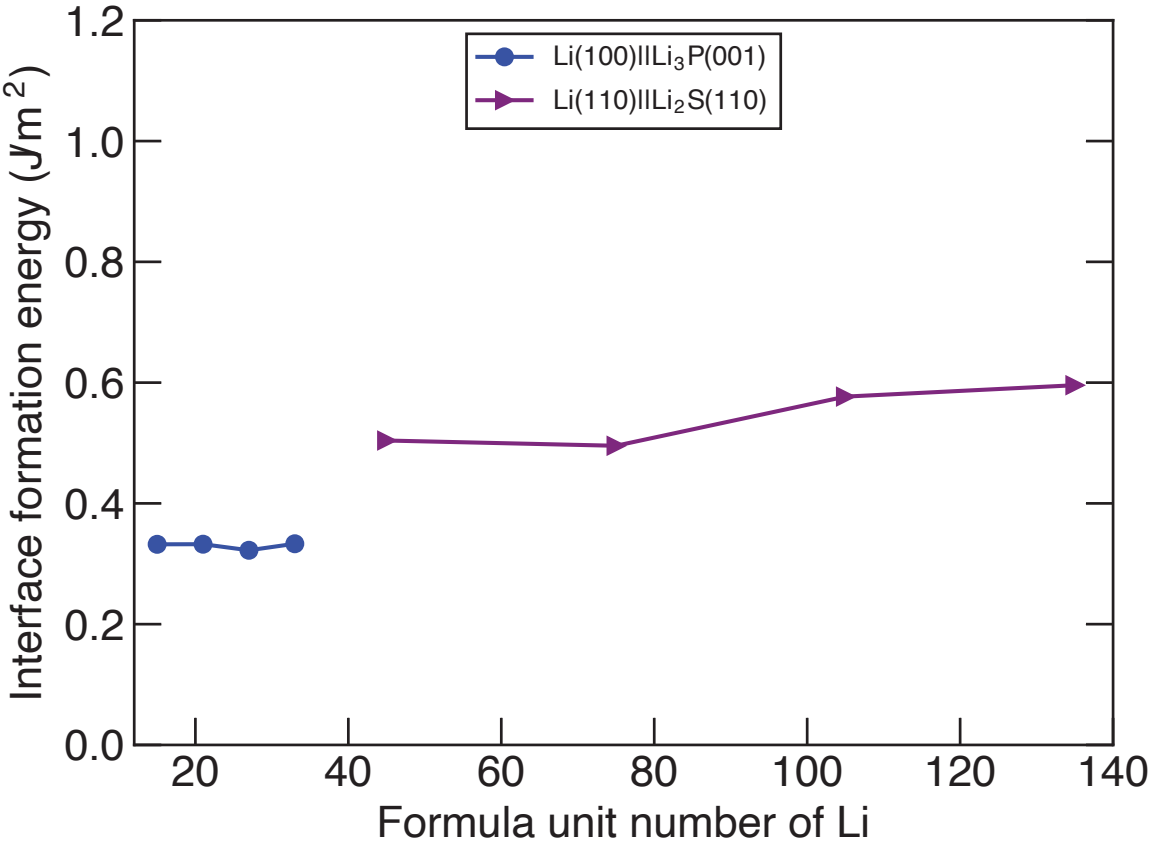

Figure S10: The calculated interface formation energy E_f (in J m^{-2}) of Li(100)||Li_3P(001) and Li(110)||Li_2S(110) interfaces using different formula units of Li-metal slab (n_{Li})

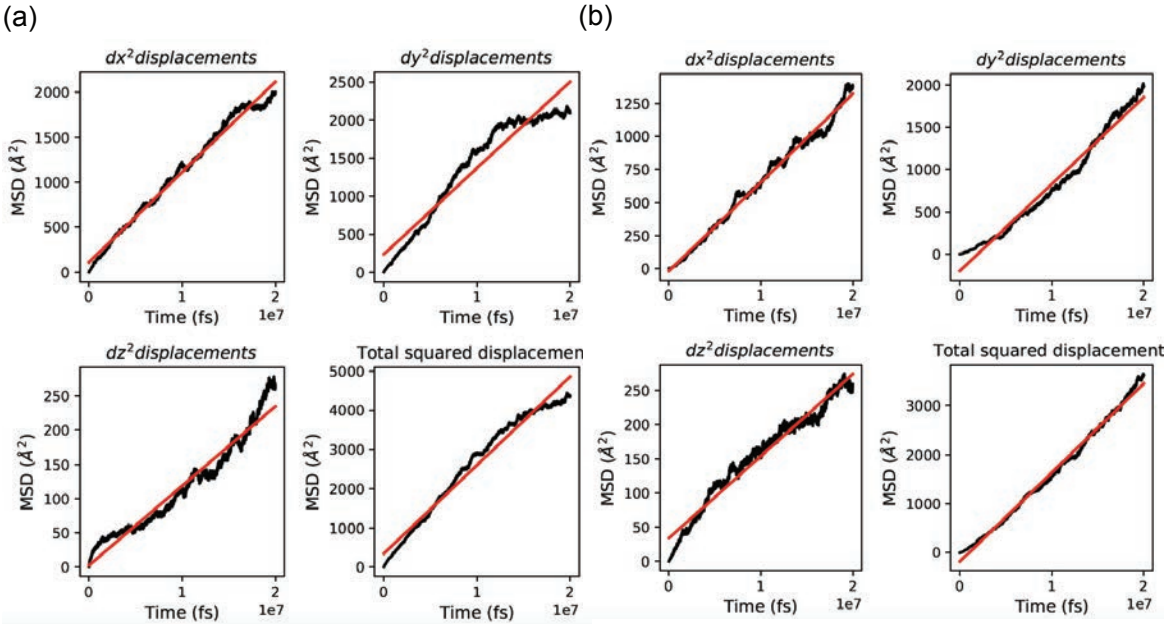

Figure S11: The MSD plots calculated from MTP-MD for Li(100)||Li_3P(001) interface at 400 K. (a) MSD of Li^+ in Li metal (b) MSD of Li^+ in Li_3P.

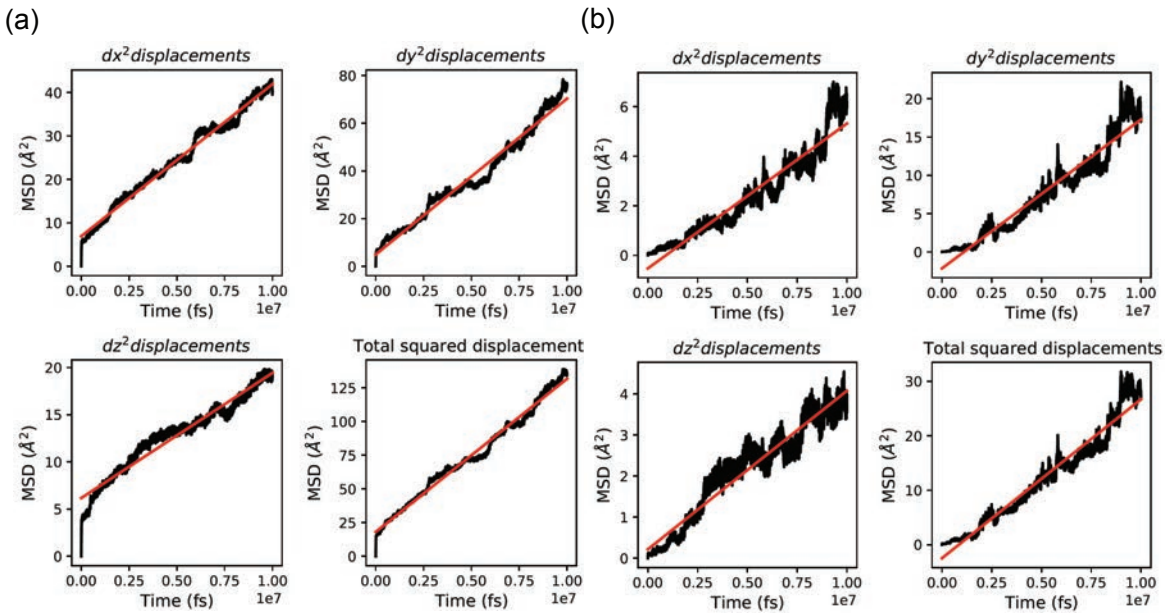

Figure S12: The MSD plots calculated from MTP-MD for Li(110)||Li_2S(110) interface at 400 K. (a) MSD of Li^+ in Li metal (b) MSD of Li^+ in Li_2S.

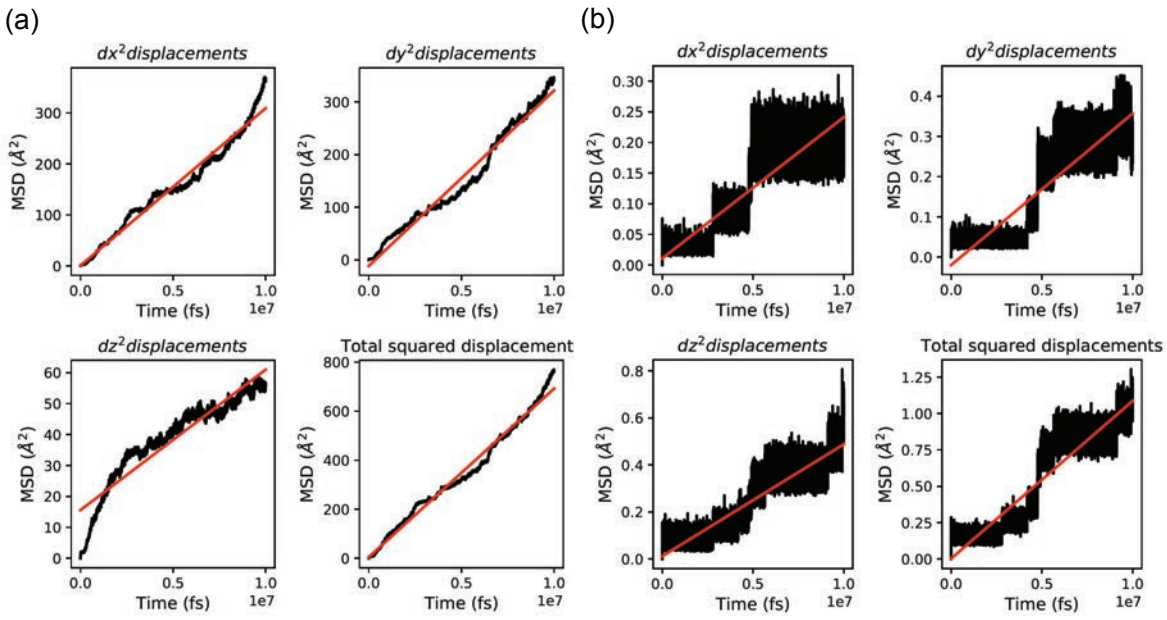

Figure S13: The MSD plots calculated from MTP-MD for Li(110)||LiCl(100) interface at 400 K. (a) MSD of Li^+ in Li metal (b) MSD of Li^+ in LiCl.

References

(1) Altorfer, F.; Bührer, W.; Anderson, I.; Schärpf, O.; Bill, H.; Carron, P.; Smith, H. Lithium diffusion in the superionic conductor Li2S. *Physica B: Condensed Matter* **1992**, *180-181*, 795–797.

(2) Nazri, G. Preparation, structure and ionic conductivity of lithium phosphide. *Solid State Ionics* **1989**, *34*, 97–102.

(3) Court-Castagnet, R.; Kaps, C.; Cros, C.; Hagenmuller, P. Ionic conductivity-enhancement of LiCl by homogeneous and heterogeneous dopings. *Solid State Ionics* **1993**, *61*, 327–334.